PROCEEDINGS, 51st Workshop on Geothermal Reservoir Engineering
Stanford University, Stanford, California, February 9-11, 2026
SGP-TR-230

Techno-Economic Feasibility of Geothermal Deep Direct-Use Systems in Grimes County, Texas

Yuxing Wu[1*], Hyunjun Oh[2], Guizhong Chen[3], Saeed Salehi[1], Chuck L. Wright[3]

1. Southern Methodist University, Dallas, Texas, USA
2. National Laboratory of the Rockies, Golden, Colorado, USA
3. NOV Inc., Houston, Texas, USA

* yuxingw@smu.edu

Keywords: Direct-Use Geothermal Systems, Techno-Economic Analysis, Reservoir Simulation, Geothermal Energy

ABSTRACT

This study evaluates the techno-economic feasibility of a deep direct-use geothermal system in Grimes County, Texas. The system consists of a doublet system, including an injector and a producer. Fluid is extracted from the subsurface for heat utilization at surface facilities and is reinjected as cooled fluid. A numerical model is developed to simulate the performance of the doublet system. The simulation time is 30 years for analyzing long-term behavior. A deep formation - the Austin Chalk, with formation top ranges from 13,000 ft (3,962 m) to 15,500 ft (4,724 m) of true vertical depth (TVD) - is selected as the reservoir formation due to the favorable sealability of the Midway and Taylor shales above. The permeable layer is sandwiched between low-permeable formations. The reservoir is assumed to be brackish water, without any hydrocarbons. Techno-economic analysis is conducted to assess economic feasibility. The sensitivity of formation characteristics such as porosity and permeability can also be modeled to examine the reservoir impact on energy production. The results of the reservoir simulation evaluate the dynamic performance of the direct-use geothermal system. Produced temperature profile, changes in reservoir pressure over time, and the amount of energy stored are simulated. Techno-economic analysis incorporates simulation results to assess the economic indicators, such as the levelized cost of energy. Additionally, the evaluation considers both technical and economic performance to provide a comprehensive assessment.

1. INTRODUCTION

The rapid expansion of geothermal energy, if intensively deployed and cooperated with other resources, is beneficial for reducing carbon footprints, diminishing grid dependence, achieving reliable and resilient energy systems, and optimizing energy generation. Direct-use geothermal systems have potential applications in heating, industrial processes, and agriculture. Compared to conventional heating technologies (e.g., fossil-fuel–based heating systems), direct-use systems are a continuous, low-emission energy resource. Over the years, several studies have been published on the regional geothermal potential of the Gulf Coast, Texas, at the basin scale as well as the county scale (Esposito & Augustine, 2012, Richards, 2020, Richards & Blackwell, 2012). However, geothermal gradient, reservoir permeability and porosity, well depth, and well construction costs limit the commercial deployments.

Recent research focused on innovative concepts, such as repurposing oil and gas wells, heat production enhancements, and well optimizations. Mohamed et al. (2022) investigated a case study in Oklahoma to repurpose abandoned oil and gas wells for direct-use applications in low-enthalpy areas. According to the results, producing 2,000 bbl/day of water was sufficient to provide energy for three public schools at an LCOH of $12.8/MMBTU. The relatively low costs showed that direct-use systems can be a cost-effective solution for energy supply. Aydin and Merey (2020) assessed the potential of geothermal energy production from a depleted gas field in Dodan, Turkey. Brine with 200 kJ/kg to 350 kJ/kg specific energy was produced to the surface for green housing, agricultural drying, and district heating applications. Monte Carlo simulations estimated that more than 9 MWt of geothermal energy can be extracted from the field.

Performance of shallow- and medium-depth geothermal wells is evaluated. Khankishiyev et al. (2024a, 2024b) evaluated the performance of supercritical CO2 in a multilateral closed-loop system. The paper highlighted the most influential factors impacting well design on system efficiency, revealing optimal flow rates and the importance of insulated tubing to prevent heat loss. After 20 years of production, the system can still provide stable energy. Wu et al. (2023) studied geothermal storage and extraction using huff-n-puff wells. The water is injected, shut-in, and produced repeatedly. Reservoir permeability, injection temperature, and operational timing strongly influence energy recovery efficiency. Afridi et al. (2024) developed a nano-engineered geopolymer cement for geothermal applications. Thermal conductivity, shear bond strength, and compressive strength were evaluated. The lab- and large-scale experiments demonstrated that microstructure and air-void distribution significantly affected heat transfer. Welsch et al. (2016) compared more than 250 different numerical models. Borehole field layout, fluid inlet temperatures, and reservoir rock properties significantly impact efficiency.

Techno-economic analysis highlights the advantages of direct-use systems, particularly in the repurposing oil and gas projects. A recent dynamic lifecycle assessment demonstrated that using abandoned wells can reduce global warming potential by up to 24% over a 30-year lifetime relative to conventional natural gas heating, due to reduced drilling emissions and a long-term renewable energy supply (Marroquin et al., 2025). The feasibility of the direct-use systems is significantly dependent on reservoir depth, flow rate, and availability of existing wells (Oh et al., 2024).

This study focuses on a doublet system in Grimes County, Texas, evaluating long-term performance and economic analysis. A numerical reservoir model is developed to simulate the behavior of existing wells over a 30-year period. Techno-economic analysis is conducted to assess economic feasibility. The sensitivity of formation characteristics such as porosity and permeability can also be modeled to examine the reservoir impact on energy production. Key indicators such as produced temperature, stored energy, pressure behavior, and levelized cost of energy are presented.

2. METHODOLOGY

In this study, geological characterization, 3D thermal-hydraulic reservoir simulations, and techno-economic analysis are combined to assess the performance of the deep direct-use geothermal system in Texas. Numerical simulations are developed to model the long-term performance of the doublet well system based on the geological setups and reservoir properties of the target area. The impacts of porosity and permeability on the thermal recovery and pressure behaviors provide a foundation for the techno-economic evaluation.

2.1 Geological and Reservoir Characterization

A deep formation - the Austin Chalk, with formation top of 14,765 ft (4,500 m) and bottom of 15,750 ft (4,800 m) TVD - is selected as the reservoir formation due to the favorable sealability. The permeable layer is sandwiched between low-permeable formations, Navarro and EagleFord formations. The thickness of the capstone and basement is 328 ft (100 m). Figure 1 shows the geological setup of the simulation. The properties of each formation layer are presented in Table 1. The parameters serve as baseline inputs. Due to the uncertainty of the properties, the influence of reservoir rocks with variable porosities and permeabilities is studied to evaluate their effects on thermal recovery and pressure behavior. The properties studied are shown in Table 2. Two hypothetical wells (Figure 2) are utilized as the injection and production wells on the NOV Springett Technology Center premises. Both wells are assumed to have a total depth of 15,580 ft (4750 m), with perforations completed between 15,090 ft (4,600 m) and 15,420 ft (4,700 m). The well is assumed vertical. Case #1 is the base case, while Case #2-7 studied the reservoir rocks with different treatments, such as acidizing and fracturing stimulations. The reservoir is assumed to contain brackish water, with no hydrocarbons. The well is assumed to be vertical, and flashing influence (water-steam phase change) is considered.

Table 1: Rock formation properties (Bhattacharya et al., 2022, Sukumar et al., 2019).

Formation	Porosity, fraction	Permeability, md	Permeability anisotropy	Thermal conductivity, W/m/K	Heat capacity, kcal/kg/K
Navarro	0.05	0.02	2.15	2.05	0.249
Austin Chalk	0.08	0.1	1.22	2.46	0.228
EagleFord	0.07	0.01	2.45	1.92	0.256

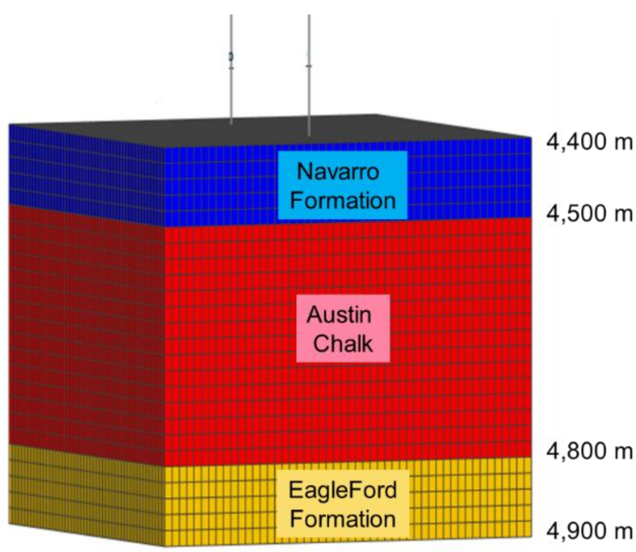

Figure 1: Geological setups of the simulations.

Table 2: Variable properties of the studied reservoir rock.

Case #	Treatment	Porosity, fraction	Permeability, md	Permeability anisotropy	Thermal conductivity, W/m/K	Heat capacity, kcal/kg/K
1	Austin chalk	0.08	0.1	1.22	2.46	0.228
2	Acidizing	0.096	0.12	1.22	2.46	0.228
3	Acidizing	0.16	0.2	1.22	2.46	0.228
4	Acidizing	0.24	1	1.22	2.46	0.228
5	Acidizing	0.32	10	1.22	2.46	0.228
6	Fracturing	0.35	50	1.22	2.46	0.228
7	Natural fractures	0.40	446.7	1.22	2.46	0.228

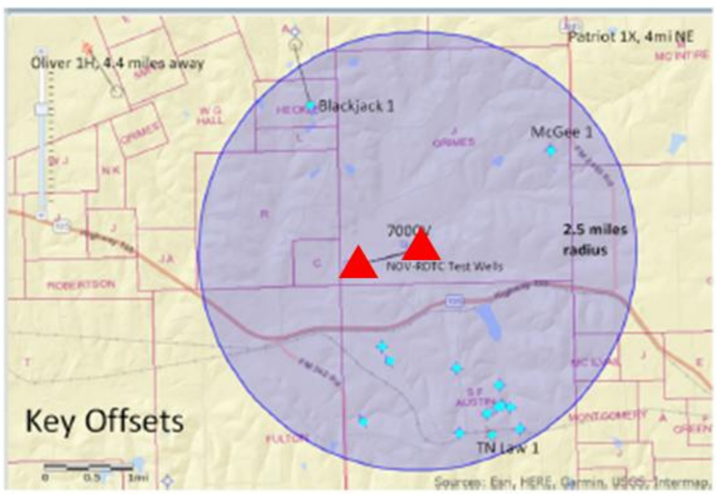

Figure 2: Location of the studied wells.

2.2 Numerical Model Development

A 3D numerical reservoir simulation model is developed by t-Navigator, to estimate the performance of the direct-use system, coupling fluid flow and heat transport behaviors. The model consists of one injector and one producer, located in the Austin Chalk formation. The well configurations are the same as Chen et al. (2023). Brackish water at 158 °F (70 °C) is injected. The simulation time is 30 years, allowing the evaluation of long-term capacity, heat breakthrough, and pressure sustainability. Based on the reported geothermal gradient, the bottom hole formation temperature is around 355 °F (180 °C) (USGS, 2012).

2.3 Techno-Economic Analysis

The levelized cost of heat (LCOH) is defined as a ratio of the system capital and operation and maintenance costs to the total thermal energy production (Equation 1). The LCOH is a widely used economic metric to assess the techno-economic performance of thermal energy systems under various configurations and operational scenarios (e.g., Oh et al. 2024), and this study estimated the LCOH of the seven cases summarized in Table 2. In this preliminary study, the analysis scope extended from the borehole field to a surface plant, and the key components considered included pumps, surface piping, and a heat exchanger. This study also assumed existing oil and gas wells are repurposed for the geothermal system.

$$LCOH = \frac{C_{cap} + \sum_{t=1}^{LT} \frac{C_{O\&M,t}}{(1+d)^t}}{\sum_{t=1}^{LT} \frac{E_t}{(1+d)^t}} \tag{1}$$

where $LCOH$ is levelized cost of heat ($/MWh$_{th}$), C_{capex} is capital expenditure ($), $C_{O\&M,t}$ represents the net annual operation and maintenance cost in year *t* ($), d is the real discount rate (unitless), LT is the system lifetime (years) assumed as 30 years in this study, and E_t is annual net amount of heating produced in year *t* (MWh$_{th}$). The useful thermal energy produced from the geothermal system was estimated using Equation 2:

$$Q = m \times C_p \times \Delta T \tag{2}$$

where Q is the heat transfer rate (W); m is the mass flow rate (kg/s); C_p is the specific heat (J/kg·K) assumed as 4,200 J/kg·K; and ΔT represents a difference in temperatures at injection and production wells obtained from numerical modeling.

Akindipe and Witter (2025) estimated the drilling cost of geothermal wells with small diameters (8.5 in. borehole and 7 in. slotted liner), which is roughly comparable to typical oil and gas well diameters, at $6–7 million for a depth of 4.7 km. For the purposes of a high-level techno-economic analysis, it was assumed that repurposing existing oil and gas wells would cost approximately 25% of the drilling cost, reflecting expenses associated with well recompletion, integrity remediation, and installation of geothermal-specific completions rather than full drilling. Based on this assumption, the CAPEX for repurposing the two wells was estimated at $3.3 million. CAPEX of the pump used to circulate fluid through the well field was estimated using an empirical correlation derived for a production pump and driver in a single geothermal production well (Mines 2016):

$$CAPEX_{pump} = \$1750 \times (P_{hp})^{0.7} + \$5750 \times (P_{hp})^{0.2} \times PPI_{pump} \tag{3}$$

where P_{hp} represents pump power in horsepower, converted from the pumping power (in watts) multiplied by 1.34. The pumping power was estimated using Equation 4:

$$P_{pump} = \frac{q \times \Delta P_{wells}}{\eta} \tag{4}$$

where P_{pump} is the pumping power (W); q is the volumetric flow rate (m^3/s) estimated in the numerical modeling for a specific amount of energy production or storage regarding porosities and permeabilities of the seven scenarios in Table 2; η is the pump efficiency assumed as 80%; and ΔP_{wells} is the pressure drop (Pa), obtained from the numerical modeling results. A pump lifetime of 20 years was assumed, and the replacement cost (the estimated CAPEX) was incorporated into the lifetime operation and maintenance cost estimation. The surface piping length between the surface plant and two wells was assumed as 500 m (250 m for each). A unit cost of $519.8/m was adopted for piping CAPEX estimation (Oh et al. 2025). Annual maintenance costs, such as leaks, corrosion, and minor repairs, were assumed to be 3% of the piping CAPEX, assuming no major failures requiring replacement over the system lifetime. Similarly, this study assumed a plate and frame heat exchanger is in the surface plant and properly functioning over 30 years. CAPEX of the heat exchanger was assumed to be $2,221.1 per kg/s ($140/gpm), with annual maintenance costs assumed to be 5% of the initial CAPEX to account for cleaning and routine servicing (Oh et al. 2025).

3. RESULTS

3.1 Reservoir Performance

Figure 3 shows the bottom-hole temperature (BHT) for 7 cases with different reservoir permeabilities and porosities over a 30-year simulation period. For low-permeability cases (ϕ≤32%, k≤ 10 md), BHT remains stable, indicating limited heat depletion within the wellbore. Thermal recovery is sustainable. In contrast, high- and moderate-permeability cases (ϕ = 35%, k = 50 md; and ϕ = 40%, k = 446 md) result in a noticeable reduction in BHT with production. The temperature decreases to 165–170 °C at the end of the simulation, reflecting a stronger thermal breakthrough effect and low heat retention efficiency.

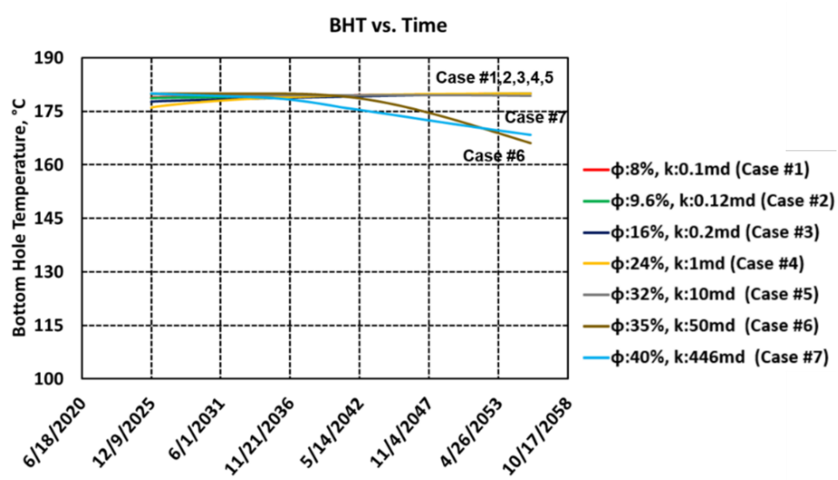

Figure 3: Bottom-hole temperature (BHT) of the production well during simulation time.

Figure 4 highlights the change in bottom-hole pressure (BHP). The reservoirs with low permeability (ϕ = 8–32%, k = 0.1–10 md) have a stable BHP behavior, with BHP remaining around 1500 psi. When the permeability is 50 md and porosity is 35%, the BHP changes to 3400 psi. The stable BHP allows long-term production without excessive depletion. High-permeability case (ϕ = 40%, k = 446 md) presents a sharp initial BHP drop from 4200 psi to 1500 psi. After 15 years of pressure drop, the BHP is stable at 1500 psi. The reason for getting higher BHP at high permeabilities is that the high-permeability cases have a much higher liquid/steam ratio in the production stream than the low-permeability case.

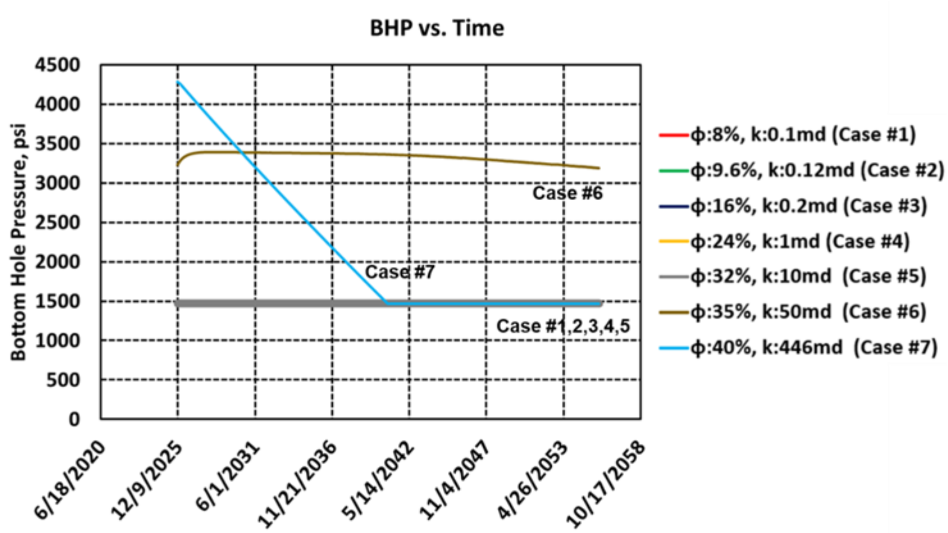

Figure 4: Bottom-hole pressure (BHP) of the production well during simulation time.

Profile of BHP in the injection well (Figure 5) illustrates that for a low-permeability reservoir (ϕ = 8–32%, k = 0.1–10 md), the injection BHP remains high and stable at 11000 psi. For mid-permeable formation (ϕ=35%, k=50md), BHP stabilizes at a lower BHP, 9300 psi. Minor pressure fluctuation occurs due to transient thermal–hydraulic interactions. The high-permeable formation (ϕ = 40%, k = 446 md) shows a significant bottomhole injection pressure decline during the early years, reducing from 4000 psi to 1200 psi. The reduction affects long-term production efficiency.

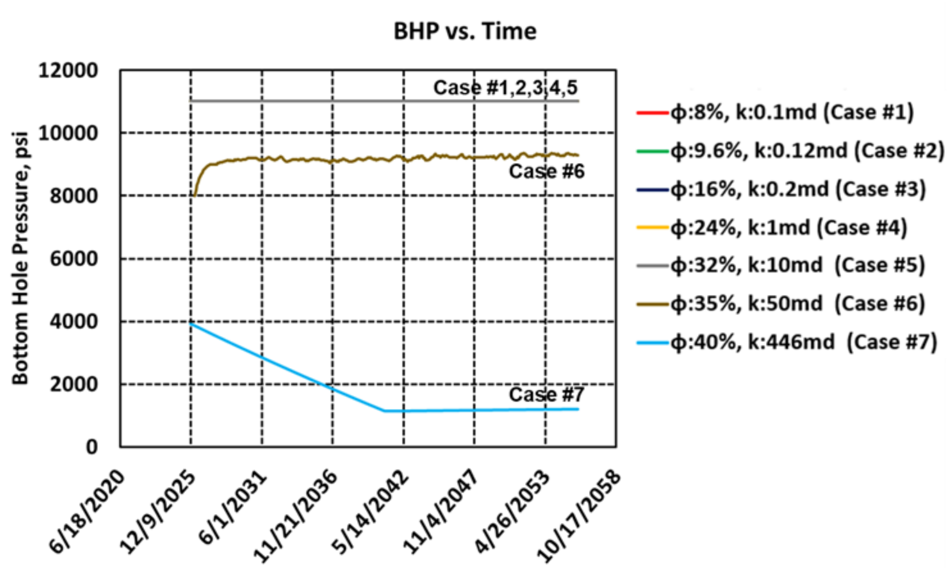

Figure 5: Bottom-hole pressure (BHP) of the injection well during simulation time.

Figure 6 illustrates the production rate changing over 30 years. For low-permeability reservoirs (Cases #1–5; ϕ = 8–32%, k = 0.1–10 md), production rates are extremely low. Production from the reservoirs provides a stable but insufficient energy supply. The mid-permeability case (Case #6; ϕ = 35%, k = 50 md) has a higher and stable production rate, 6000-7000 sm3/day. A favorable balance between injection and flow resistance is generated to maintain reservoir pressure and thermal stability. The production rate of the high-permeability case (Case #7; ϕ = 40%, k = 446 md) is high, around 24000 sm3/day. A significant drop is observed at the beginning of the production and maintains around 2500 sm^3/day, indicating an energy production and low efficiency during long-term operations.

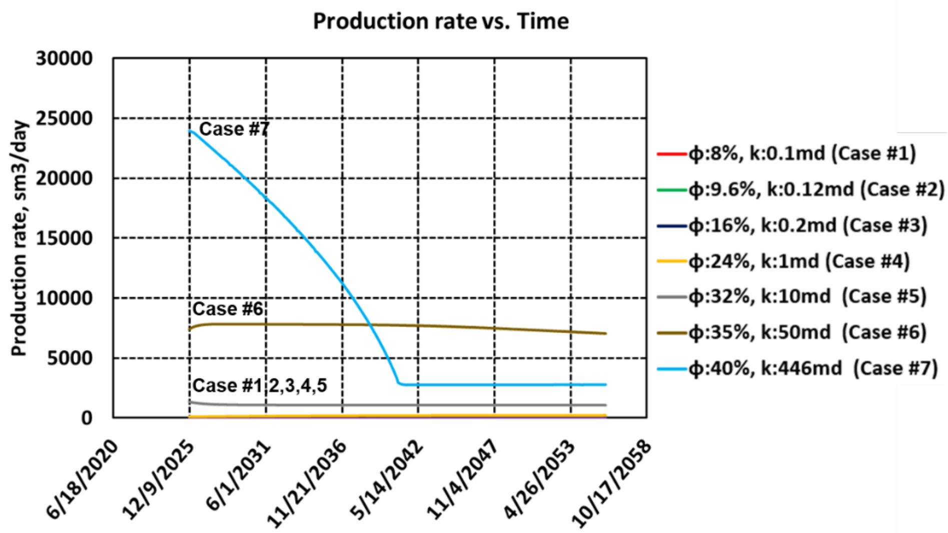

Figure 6: Production rate changing during simulation time.

Figure 7 is the outlet pressure changing with time. For low-permeability cases (Cases #1–5; ϕ = 8–32%, k = 0.1–10 md), the outlet temperature is stable and high. However, due to the low production rate, the reservoirs provide insufficient energy. The outlet temperature of the mid-permeability case (Case #6; ϕ = 35%, k = 50 md) remains at 179 °C at the beginning and drops to 166 °C, representing limited thermal breakthrough, while remaining at a high production temperature. The high-permeable case shows the largest and earliest decrease in temperature. The decline shows severe thermal depletion and low long-term efficiency.

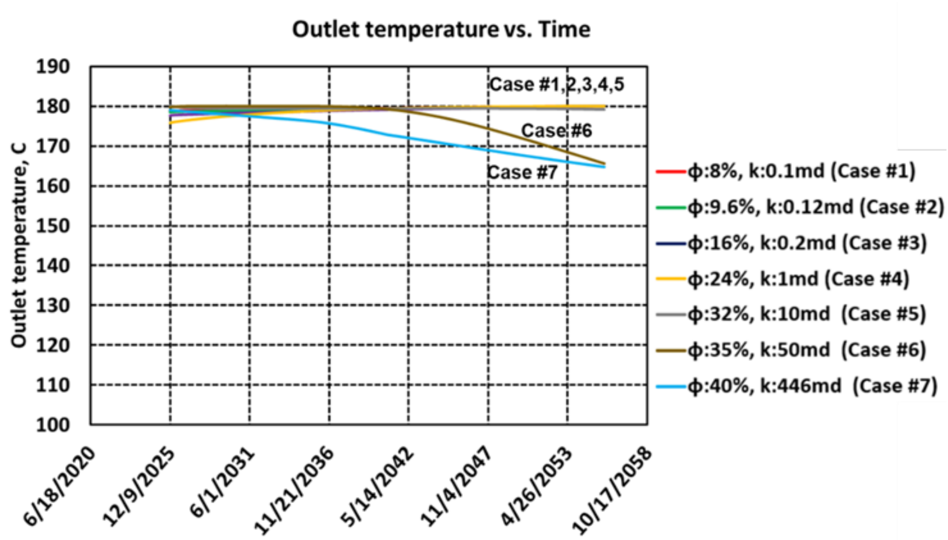

Figure 7: Outlet temperature (the temperature at the casing outlet in the production well) changing during simulation time.

3.2 Techno-Economic Analysis

Table 3 summarizes the CAPEX, annual O&M costs, and LCOH for the seven cases. Pump CAPEX, which was based on pumping power (Equation 3), showed strong sensitivity to reservoir pressure changes governed by reservoir porosity, permeability, and flow rate. As discussed earlier with Figures 3 and 4, cases with lower reservoir porosity and permeability exhibited larger bottomhole pressure differences between the injection and production wells, leading to higher pumping power, and consequently, substantially higher pump CAPEX and associated operating costs. In contrast, Case 7, characterized by high permeability, presented significantly lower pressure differences, resulting in reduced pumping requirements and correspondingly lower pump CAPEX and OPEX. Although heat exchanger CAPEX increased with higher flow rates and thermal duties, its contribution to total CAPEX remained relatively small in the lower-cost cases and became significant only in Cases 6 and 7. Surface piping CAPEX was held constant across all cases and thus did not contribute to the observed cost variations.

Table 3. Summary of economic metrics for the seven cases

	Case 1	Case 2	Case 3	Case 4	Case 5	Case 6	Case 7
Total CAPEX (USD, $)	297k	304k	329k	483k	960k	2 million	1.4 million
Annual O&M cost (USD, $)	12k	14k	26k	143k	1.6 million	5.1 million	1.2 million
LCOH ($/MWh$_{th}$)	175.5	131.9	68.9	36	31.6	18.8	1.4

The combined effects of pumping and heat exchanger costs were reflected in the total CAPEX and annual O&M costs. Total CAPEX increased from approximately $300k in Case 1 to $2 million in Case 6, driven primarily by escalating pumping requirements. Similarly, annual O&M costs were dominated by pumping energy consumption, while maintenance costs were assumed to be identical across all cases. These cost trends directly affected the LCOH, which decreased monotonically from 175.5 $/MWh$_{th}$ in Case 1 to 18.8 $/MWh$_{th}$ in Case 6, reaching a minimum value of 1.4 $/MWh$_{th}$ in Case 7. Despite its favorable pumping economics (due to the high permeability), the low LCOH of Case 7 should be interpreted with caution, as thermal energy production declines substantially after approximately 10 years of operation (Figure 5), which may limit its long-term economic viability.

4. DISCUSSION

The study evaluates the performance of a deep direct-use system based on reservoir assessments, bottom-hole behaviors, and production responses, rather than heat flux, to directly reflect the energy extracted to the surface. Previous studies have highlighted heat flux and transfer, as well as instantaneous heat extraction rates, to characterize reservoir performance (Diersch & Bauer, 2021, Ghoreishi-Madiseh et al., 2015, Moradi et al., 2015). From a long-term production perspective, BHT, BHP, production rates, and outlet temperature are more closely aligned with the determination of feasibility. Additionally, due to geological heterogeneity and stimulation operations, models with a single formation property cannot accurately represent the field conditions. Therefore, data uncertainty is investigated. The study compares the properties with several formation treatments, including acidizing, hydraulic fracturing, and the presence of natural fractures.

Simulation results show that permeability is important to balance the thermal decline and long-term production. For low-permeable formations ($\phi \leq 32\%$, $k \leq 10$ md), BHT and outlet temperature are high, while insufficient energy is extracted from the reservoir. For the high-permeable formation ($\phi = 40\%$, $k = 446$ md), the initial production is high, while the pressure drops and a significant breakthrough occurs, indicating that high permeability dissipates the stored energy and cannot maintain the long-term production. The mid-permeable formation, with 35% porosity and 50 md permeability, demonstrates the most balanced performance. A stable BHP and BHT, minor temperature decline, and relatively higher outlet temperature can provide sustainable production.

It is also important to note that Case 7, with extremely high permeability, yields the lowest LCOH because of the significantly high geothermal energy production in the early stages. However, the scenario is highly uncertain. The rapid pressure drop and fast thermal breakthrough cause a reduction in flow rates. Therefore, the scenario represents an idealized upper-limit scenario rather than a realistic operational configuration. In contrast, Case 6 balances production performance and economic outcomes. The stable flow rates, relatively high BHP, and sustained outlet temperature contribute to a

reliable long-term heat supply.

5. SUMMARY AND CONCLUSIONS

The study evaluates the thermal-hydraulic behavior and techno-economic analysis of deep direct-use systems with varying reservoir properties. A numerical reservoir simulation is developed to model the bottom-hole temperature and pressure behavior, injection and production rates, and outlet temperature response. The following are the details of the finding:

- Low-permeable reservoirs ($\phi \leq 32\%$, $k \leq 10$ md) generate stable BHTs and outlet temperatures, indicating a strong heat retention but insufficient production rates.
- Mid-permeable reservoir ($\phi = 35\%$, $k = 50$ md) has a stable BHP, allowing long-term production.
- High-permeable reservoir ($\phi = 40\%$, $k = 446$ md) generates a high initial production rate and BHP and quick drops after 10 years. The reduction reflects strong heat breakthrough effects and low long-term efficiency.
- Techno-economic analysis shows that pumping requirements are the dominant cost driver for both system CAPEX and annual O&M costs, primarily due to their strong dependence on reservoir pressure drops governed by porosity, permeability, and flow rate. Correspondingly, the LCOH spans a wide range across the seven cases, decreasing substantially with reduced pumping demand and increased energy production.
- According to the preliminary analysis, the mid-permeability scenario ($\phi = 35\%$, $k = 50$ md) emerges as the optimal case, providing stable production performance and sufficient energy output.

ACKNOWLEDGMENTS

The authors would like to express their sincere appreciation to Rock Flow Dynamics (RFD) company for providing the reservoir simulator t-Navigator. Additionally, thanks to Mr. Edward Evans and Mr. Luis Gracian for their support on the simulations.

NOMENCLATURE

Acronyms

BHP	Bottom-hole pressure
BHT	Bottom-hole temperature
LCOH	Levelized cost of heat
TVD	True vertical depth
gpm	Gallon per minute

Symbols

ΔP_{wells}	Pressure drop
$C_{O\&M,t}$	Net annual operation and maintenance cost in year t
E_t	Annual net amount of heating produced in year t
P_{hp}	Pump power
ΔT	Difference in temperatures at injection and production wells
C_{cap}	Capital expenditure
C_p	Specific heat
d	Real discount rate
K	Permeability
LT	Lifetime
m	Mass flow rate
Q	Heat transfer rate
q	Volumetric flow rate
η	Pump efficiency
Φ	Porosity

REFERENCES

Afridi, M. A., Wu, Y., Khattak, M. J. & Karbalaeisaleh, F.: Development of a highly conductive nano-engineered geopolymer for geothermal applications. ASME Open Journal of Engineering 3 (2024), 031031.

Akindipe, D., & Witter, E.: Geothermal drilling cost curves updates, Proceedings, 50th Workshop on Geothermal Reservoir Engineering, Stanford University, Stanford, CA (2025).

Aydin, H. & Merey, S.: Potential of geothermal energy production from depleted gas fields: A case study of Dodan Field, Turkey. Renewable Energy 164 (2021): 1076-1088.

Chen, G., Wright, C., Nelson, C., Stuart, G., Wang, P.: An updated geomechanical model for an innovation test well drilled at a drilling test facility in Grimes County, Texas. ARMA 23-0063 (2023).

Diersch, H.-J. G. & Bauer, D.: Analysis, modeling, and simulation of underground thermal energy storage systems. Elsevier: Advances in Thermal Energy Storage Systems (2021), 173-203.

Esposito, A. & Augustine, C.: Recoverable resource estimate of identified onshore geopressured geothermal energy in Texas and Louisiana (Presentation). (2012).

Ghoreishi-Madiseh, S. A., Sasmito, A. P., Hassani, F. P. & Amiri, L.: Heat transfer analysis of large scale seasonal thermal energy storage for underground mine ventilation. Energy Procedia 75 (2015), 2093-2098.

Khankishiyev, O., Hasanov, G., Ismayilov, E., Wu, Y., Karami, H. & Salehi, S.: Evaluation of multilateral well design and sco2 for closed loop geothermal systems. 2024 Geothermal Rising Conference (2024a), 72-95.

Khankishiyev, O., Wu, Y., Karami, H., Salehi, S. & Farajli, H.: Potential of multilateral closed loop geothermal systems for power generation using water and supercritical CO2. SPE Europec featured at EAGE Conference and Exhibition (2024b).

Marroquin, I., Oh, H., Ghosh, T., Hu, Z., Salehi, S., Nygaard, R.: Dynamic life cycle assessment for evaluating the global warming potential of geothermal energy production using inactive oil and gas wells for district heating in Tuttle, Oklahoma. Science of the Total Environment 970 (2025), 178932.

Mohamed, A., Ugarte, E., Vivas, C., Wu, Y., Cedola, A. & Salehi, S.: Repurposing abandoned oil and gas wells for geothermal direct use in Oklahoma: A case study. Geothermal Resources Council Transactions (2022), 72-82.

Moradi, A., Smits, K. M., Massey, J., Cihan, A. & McCartney, J.: Impact of coupled heat transfer and water flow on soil borehole thermal energy storage (SBTES) systems: Experimental and modeling investigation. Geothermics 57 (2015), 56-72.

Oh, H., Akar, S., Beckers, K., Bonnema, E., Vivas, C., Salehi, S.: Techno-economic feasibility of geothermal energy production using inactive oil and gas wells for district heating and cooling systems in Tuttle, Oklahoma. Energy Conversion and Management 308 (2024): 118390.

Oh, H., Jin, W., Peng, P., Winick, J. A., Sickinger, D., Sartor, D., Zhang, Y., Beckers, K., Kitz, K., Acero-Allard, D., Atkinson, T.A., and Dobson, P.: Techno-economic performance of reservoir thermal energy storage for data center cooling system, Applied Energy, 391 (2025), 125858.

Richards, M. C., Blackwell, D. D.: Developing geothermal energy in Texas: mapping the temperatures and resources. (2012).

Richards, M.: Analysis of geothermal resources in three Texas counties. USDOE Geothermal Data Repository (2020).

USGS, 2012. Temperature and Petroleum Generation History of the Wilcox Formation, Louisiana. Report: 2012–1046.

Welsch, B., Rühaak, W., Schulte, D. O., Bär, K. & Sass, I.: Characteristics of medium deep borehole thermal energy storage. International Journal of Energy Research 40 (2016), 1855-1868.

Wu, Y., Salehi, S. & Karbalaeisaleh, F.: Numerical investigation of geothermal storage and extraction using huff-n-puff wells. US Rock Mechanics/Geomechanics Symposium, ARMA-2023-0494 (2023).